Inorg. Chem. **2008**, *47*, 1687−1692

On the Anisotropy of the Magnetic Properties of $CsYbZnSe_3$

George H. Chan,[†] Changhoon Lee,[‡] Dadi Dai,[‡] Myung-Hwan Whangbo,[*,‡] and James A. Ibers[*,†]

Department of Chemistry, Northwestern University, 2145 Sheridan Road, Evanston, Illinois 60208-3113, and Department of Chemistry, North Carolina State University, Raleigh, North Carolina 27695-8204

Received October 4, 2007

DC magnetic susceptibility measurements on $CsYbZnSe_3$ show a broad magnetic transition at ≈10 K and pronounced differences between zero-field-cooled and field-cooled data that lead to experimental effective magnetic moments of 4.26(5) BM and 4.39(4) BM, respectively. Specific heat measurements confirm that there is neither long-range ordering nor a phase transition between 1.8 and 380 K. First-principles electronic structure calculations with and without inclusion of spin–orbit coupling effects show that the spins of $CsYbZnSe_3$ prefer to orient along [010] rather than along either [100] or [001] of this orthorhombic material and that the spin exchange between adjacent Yb^{3+} ions along [100] is substantially antiferromagnetic. The magnetic properties of $CsYbZnSe_3$ are best described by an Ising uniform antiferromagnetic chain model.

Introduction

The isostructural $ALnMQ_3$ materials (A = Rb, Cs; Ln = rare-earth metal; M = Mn, Co, Zn, Cd, Hg; Q = S, Se, Te) are a class of magnetic semiconductors with tunable optical band gaps.[1−5] Previous experiments and first-principles electronic structure calculations indicated that the band gaps of these materials can be tuned through simple chemical substitution of Ln, M, or Q.[1−4] For some of these compounds there is also a slight dependence of band gap on crystal orientation.[3,4] The $ALnMQ_3$ compounds are mostly normal Curie–Weiss paramagnets, but those containing Yb^{3+} (Table 1), that is, $CsYbZnS_3$, $RbYbZnSe_3$, $CsYbZnSe_3$, and $CsYbMnSe_3$, exhibit a broad maximum at $T_{max} \approx 10$ K in their magnetic susceptibility and pronounced differences between zero-field-cooled (ZFC) and field-cooled (FC) magnetic data.[3] These compounds have negative values of the Weiss temperature θ, which indicates that the dominant spin-exchange interactions are antiferromagnetic (AFM);[3,5] the broad susceptibility maximum at ≈10 K indicates the presence of short-range AFM order.[3] The latter is typically found for magnetic solids with low-dimensional spin lattices of spin $-^1/_2$ ions, for example, isolated spin dimer and Heisenberg uniform AFM chain systems.[6]

Table 1. Shortest Yb-Yb Distances[a] and Magnetic Data for $AYbMQ_3$ Materials

compound	Yb−Yb (Å)	μ_{eff} (BM)	T_{max} (K)	θ (K)	reference
$CsYbCoS_3$	3.9317(4)	5.85(1), ZFC	≈2.7	−102.5(1)	5
$CsYbZnS_3$	3.9543(5)	4.72(1)	≈10	−26.6(6)	3
$CsYbCoSe_3$	4.0669(3)				5
$RbYbZnSe_3$	4.0737(4)	4.81(5)	≈10	−22.3(2)	3
$CsYbZnSe_3$	4.0853(4)	4.64(2)	≈10	−50.2(2)	4
$CsYbZnSe_3$	4.087(1),	4.26(5), ZFC	≈10	−34.3(3)	this work
	4.107(5)[b]	4.39(4), FC	≈11	−25.4(2)	
$CsYbMnSe_3$	4.1447(8)	6.83(2)	≈10	−89.9(4)	3
$RbYbZnTe_3$	4.3228(5)				3
$CsYbZnTe_3$	4.3377(6)				3

[a] This distance is the length of the *a* axis. [b] Unit cell determined at 298 K; all other unit cells were determined at 153 K.

AC susceptibility measurements and a neutron diffraction study indicate that $CsYbZnSe_3$, a representative member the $AYbMQ_3$ compounds that exhibit the broad magnetic transi-

* To whom the mail to correspondence should be addressed. E-mail: ibers@chem.northwestern.edu (J.A.I.), mike_whangbo@ncsu.edu (M.-H.W.).
[†] Northwestern University.
[‡] North Carolina State University.

(1) Mitchell, K.; Huang, F. Q.; McFarland, A. D.; Haynes, C. L.; Somers, R. C.; Van Duyne, R. P.; Ibers, J. A. *Inorg. Chem.* **2003**, *42*, 4109–4116.
(2) Yao, J.; Deng, B.; Sherry, L. J.; McFarland, A. D.; Ellis, D. E.; Van Duyne, R. P.; Ibers, J. A. *Inorg. Chem.* **2004**, *43*, 7735–7740.
(3) Mitchell, K.; Huang, F. Q.; Caspi, E. N.; McFarland, A. D.; Haynes, C. L.; Somers, R. C.; Jorgensen, J. D.; Van Duyne, R. P.; Ibers, J. A. *Inorg. Chem.* **2004**, *43*, 1082–1089.
(4) Mitchell, K.; Haynes, C. L.; McFarland, A. D.; Van Duyne, R. P.; Ibers, J. A. *Inorg. Chem.* **2002**, *41*, 1199–1204.
(5) Chan, G. H.; Sherry, L. J.; Van Duyne, R. P.; Ibers, J. A. *Z. Anorg. Allg. Chem.* **2007**, *633*, 1343–1348.
(6) (a) Kahn, O. *Molecular Magnetism*; VCH Publisher: Weinheim, 1993. (b) Johnston, D. C.; Kremer, R. K.; Troyer, M.; Wang, X.; Klümper, A.; Bud'ko, S. L.; Panchula, A. F.; Canfield, P. C. *Phys. Rev. B: Condens. Matter* **2000**, *61*, 9558–9606.

10.1021/ic701961f CCC: $40.75
Published on Web 02/08/2008

tions, is neither a spin-glass nor does it exhibit long-range ordering.[3] To gain insight on the puzzling magnetic properties of the $AYbMQ_3$ compounds, we first discuss the specific heat and magnetic susceptibility measurements on $CsYbZnSe_3$ and then clarify the nature of its magnetic susceptibility maximum at $T_{max} \approx 10$ K with the use of first-principles density functional theory (DFT) electronic structure calculations including spin–orbit coupling (SOC). We show that the Yb^{3+} ions of $CsYbZnSe_3$ are a highly anisotropic spin system and that an Ising uniform AFM chain spin–lattice model appropriately describes the magnetic properties.

Experimental Section

Synthesis and Characterization of $CsYbZnSe_3$. From a slight modification of the literature procedure[3] red needles of $CsYbZnSe_3$ were prepared in about 80% yield by the reactive flux method.[7] The heating profile used here differed slightly from that used earlier. The sample was heated to 1273 K in 48 h, kept at 1273 K for 50 h, and cooled at 4 K/h to 473 K, and then the furnace was turned off.

Energy-dispersive X-ray (EDX) analyses were carried out with the use of a Hitachi S-3500 SEM. Data were collected with an accelerating voltage of 20 keV, a working distance of 15 mm, and a collection time of 90 s. Selected single crystals of $CsYbZnSe_3$ showed the presence of Cs, Yb, Zn, and Se at an approximate ratio of 1:1:1:3. There was no evidence for the presence of I.

The unit-cell parameters of a single crystal of $CsYbZnSe_3$ were determined with a Bruker Smart 1000 CCD diffractometer[8] at both 153 and 298 K with the use of monochromatized Mo Kα radiation ($\lambda = 0.71073$ Å). The lattice parameters of this orthorhombic material are $a = 4.087(1)$ Å, $b = 15.803(9)$ Å, and $c = 10.806(5)$ Å (153 K); $a = 4.107(5)$ Å, $b = 15.89(1)$ Å, and $c = 10.82(1)$ Å (298 K). The lattice parameters at 153 K agree with those of $a = 4.0853(4)$ Å, $b = 15.7864(15)$ Å, and $c = 10.8068(10)$ Å reported previously.[3,4]

Specific Heat Measurements. The specific heat C_p of $CsYbZnSe_3$ was measured in the temperature region 1.8−260 K at applied fields of 0 and 9 T by means of a pulsed relaxation technique with the use of a Quantum Design Physical Properties Measurement System (PPMS). A total of 12.9 mg of crushed single crystals of $CsYbZnSe_3$ were pressed into a pellet that was then mounted with apiezon grease on the base of a heat capacity puck. Similar measurements of the base platform and grease without the pellet provided the background correction.

Magnetic Susceptibility Measurements. DC magnetic susceptibility measurements were carried out with the use of a Quantum Design MPMS5 SQUID magnetometer. The composition of the given sample was verified by EDX measurements. Crushed single crystals of $CsYbZnSe_3$ were ground and loaded into gelatin capsules. On a 5.5 mg sample, magnetization versus applied field was measured at 2, 10, and 15 K. In the temperature range 1.8−380 K both ZFC and FC measurements on a 6.2 mg sample were carried out with an applied field of 500 G (0.05 T). The susceptibility data were corrected for core diamagnetism.[9] The inverse molar susceptibilities χ_m^{-1} in the temperature range 50−380 K for both ZFC and FC data were fit by a least-squares method to the Curie–Weiss equation $\chi_m^{-1} = (T-\theta)/C$, where C is the Curie constant and θ is the Weiss temperature. The effective magnetic moments μ_{eff} (in BM) were calculated from the equation $\mu_{eff} = (7.997C)^{1/2}$.[10]

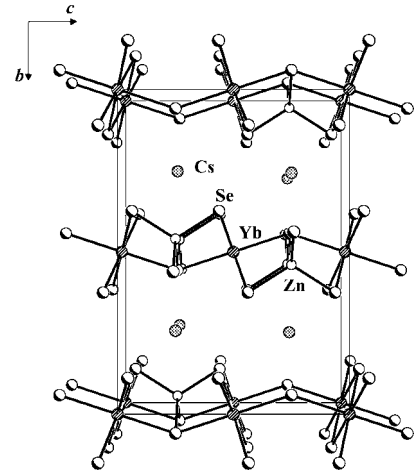

Figure 1. Unit cell of $CsYbZnSe_3$.

First-Principles Electronic Structure Calculations. The magnetic properties of $CsYbZnSe_3$ were investigated with first-principles DFT electronic structure calculations employing the full-potential linearized augmented plane wave method[11] encoded in the WIEN2k program[12] with the generalized-gradient approximation (GGA).[13] A plane-wave cutoff energy of −6.0 Ry, 20 k-points for the irreducible Brillouin zone, and $R_{MT} \cdot K_{max} = 7$ were used in the calculations. The muffin-tin radii for Yb, Cs, Se, and Zn of 2.5, 2.5, 2.15, and 2.42 au were used, respectively. The total energy converged within 10^{-5} Ry. To describe properly the strong electron correlation associated with the *f*-electrons of Yb, the GGA plus on-site repulsion U (GGA+U) method[14] was employed. The SOC on Yb was included on the basis of the second-variational method[15] using scalar relativistic wave functions by performing GGA+U+SOC calculations.

Results and Discussion

Crystal Structure. As determined earlier,[4] the compound $CsYbZnSe_3$ possesses the $KZrCuS_3$ structure type,[16] crystallizing with four formula units in space group *Cmcm* of the orthorhombic system. The unit cell of $CsYbZnSe_3$ is illustrated in Figure 1. Each Cs atom (site symmetry *mm*) is coordinated to eight Se atoms in a bicapped trigonal prismatic geometry; each Yb atom (site symmetry 2/*m*) is coordinated to six Se atoms to form a distorted octahedron; each Zn atom (site symmetry *mm*) is coordinated to four Se atoms in a distorted tetrahedral arrangement. Each $ZnSe_4$ tetrahedron shares edges with four $YbSe_6$ octahedra along [001] to form

(7) Sunshine, S. A.; Kang, D.; Ibers, J. A. *J. Am. Chem. Soc.* **1987**, *109*, 6202–6204.
(8) Bruker. *SMART*, Version 5.054 Data Collection, and *SAINT-Plus*, Version 6.45a Data Processing Software for the SMART System; Bruker Analytical X-Ray Instruments, Inc.: Madison, WI, 2003.
(9) Mulay, L. N., Boudreaux, E. A., Eds. *Theory and Applications of Molecular Diamagnetism*; Wiley-Interscience: New York, 1976.
(10) O'Connor, C. J. *Prog. Inorg. Chem.* **1982**, *29*, 203–283.
(11) Madsen, G. K. H.; Blaha, P.; Schwarz, K.; Sjöstedt, E.; Nordström, L. *Phys. Rev. B: Condens. Matter* **2001**, *64*, 1951134/1–195134/9.
(12) Blaha, P.; Schwarz, K.; Madsen, G. K. H.; Kvasnicka, D.; Luitz, J. *WIEN2k, An Augmented Plane Wave Plus Local Orbitals Program for Calculating Crystal Properties*; Vienna University of Technology, Austria, 2001; ISBN 3-9501031-1-2.
(13) Perdew, J. P.; Burke, K.; Ernzerhof, M. *Phys. Rev. Lett.* **1996**, *77*, 3865–3868.
(14) Dudarev, S. L.; Botton, G. A.; Savrasov, S. Y.; Humphreys, C. J.; Sutton, A. P. *Phys. Rev. B* **1998**, *57*, 1505–1509.
(15) Kuneš, J.; Novák, P.; Diviš, M.; Oppeneer, P. M. *Phys. Rev. B: Condens. Matter* **2001**, *63*, 205111/1–205111/9.
(16) Mansuetto, M. F.; Keane, P. M.; Ibers, J. A. *J. Solid State Chem.* **1992**, *101*, 257–264.

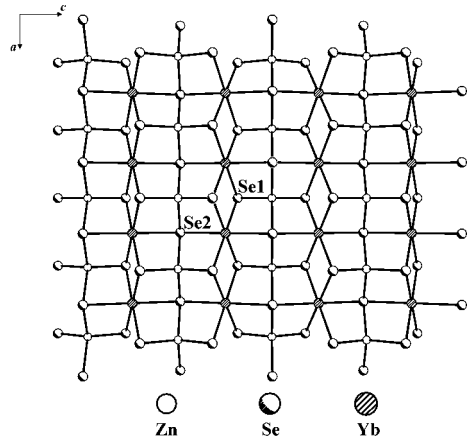

Figure 2. $^{2}_{\infty}[YbZnSe_3^-]$ layer viewed down [010].

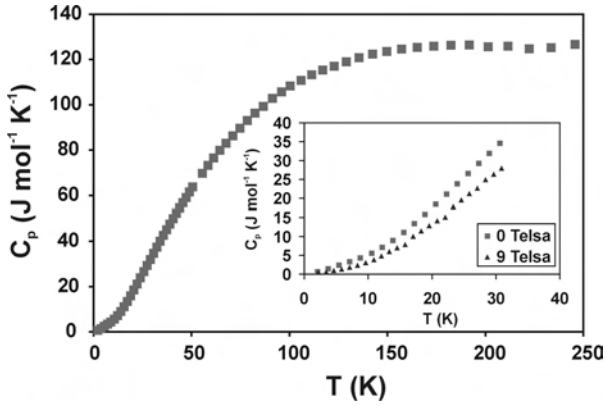

Figure 3. Specific heat C_p vs T for $CsYbZnSe_3$. Inset shows the plot of C_p vs T at low temperatures.

a two-dimensional $^{2}_{\infty}[YbZnSe_3^-]$ layer. As illustrated in Figure 2, the $^{2}_{\infty}[YbZnSe_3^-]$ layers stack perpendicular to [010] and are separated by Cs atoms. These in turn form a layer composed of face- and edge-sharing $CsSe_8$ bicapped trigonal prisms. Each $CsSe_8$ prism has two face-sharing neighbors along [100] and four edge-sharing ones along [001] to form a $^{2}_{\infty}[CsSe_3^{5-}]$ layer in the *ac* plane. Each $YbSe_6$ octahedron edge shares with two other octahedra along [100] to form a one-dimensional $^{1}_{\infty}[YbSe_4^{3-}]$ chain. The $ZnSe_4$ tetrahedra share vertices with two neighboring tetrahedra along [100] to form a one-dimensional $^{1}_{\infty}[ZnSe_3^{4-}]$ chain. Because there are no Se−Se bonds in the structure, the formal oxidation states of Cs/Yb/Zn/Se may be assigned as 1+/3+/2+/2−, respectively.

Specific Heat of $CsYbZnSe_3$. The temperature dependence of C_p was collected at applied fields of 0 and 9 T for $CsYbZnSe_3$ (Figure 3). Analyses of the low-temperature region confirm that there is neither long-range ordering nor a phase transition at or around 10 K. The results obtained here are in accord with those found in a previous neutron diffraction study.[3] In the low-temperature region, the specific heat is of the form $C_p = \gamma T + \beta T$,[3] where γ is the electronic contribution and β is the lattice contribution. The Debye temperature, Θ_D, can be estimated from the equation $\beta = (12\pi^4 n k_B)/(5\Theta_D^3)$, where k_B is the Boltzmann constant and n is the number of atoms per formula unit.[17] From the plot of C_p/T versus T^2 for the 0 T data in the temperature range 4−15 K we find $\gamma = 396$ mJ K^{-2} mol^{-1}, $\beta = 1.3$ mJ K^{-4} mol^{-1}, and $\Theta_D = 208$ K. Similar values of γ, β, and Θ_D were obtained for data collected at 9 T. Note that some Ce and Yb compounds that show heavy fermion behavior typically have $\gamma > 1$ J K^{-2} mol^{-1}.[17] Hence, it is unlikely that $CsYbZnSe_3$ is a heavy fermion material.

Magnetic Properties of $CsYbZnSe_3$. The magnetic properties of $AYbMQ_3$ (M = Mn, Zn) present several puzzling features if the spin of Yb^{3+} ($4f^{13}$; $S = {}^1/_2$; $L = 3$) is treated as a Heisenberg (i.e., isotropic) spin. For these compounds, the value of the temperature T_{max} at which the magnetic susceptibility is a maximum is nearly identical (i.e., $T_{max} \approx 10$ K). One would expect similar T_{max} values for $CsYbZnS_3$, $RbYbZnSe_3$, and $CsYbZnSe_3$ because these isostructural compounds have Yb^{3+} ions as their sole magnetic ions.

In contrast, the Weiss temperatures θ for $CsYbZnS_3$, $RbYbZnSe_3$, and $CsYbZnSe_3$ vary considerably (Table 1). For a Heisenberg uniform AFM chain defined by a nearest-neighbor spin-exchange parameter J, T_{max} is related to J as[6]

$$k_B T_{max}/|J| = 0.641 \quad (1)$$

Consequently, if the spin lattices of $CsYbZnS_3$, $RbYbZnSe_3$, and $CsYbZnSe_3$ can be described by a Heisenberg uniform AFM chain (either along the edge-sharing or the corner-sharing direction; that is, along [100] or [001], respectively), then $J/k_B \approx -16$ K when $T_{max} \approx 10$ K. According to the mean-field approximation,[18] θ for a spin lattice made up of identical spin sites is related to the sum of all the spin-exchange interactions of a given spin site as

$$\theta = [S(S+1)/3k_B]\sum_i z_i J_i \quad (2)$$

where z_i is the number of nearest neighbor spin sites connected by the spin-exchange parameter J_i. For the compounds $CsYbZnS_3$, $RbYbZnSe_3$, and $CsYbZnSe_3$, $\theta = (J_1 + J_1')/2k_B$, where J_1 and J_1' are the spin-exchange interactions between nearest-neighbor Yb^{3+} ions along the corner- and edge-sharing directions, respectively. If J_1 or J_1' is negligible, then $J/k_B = 2\theta$ (here J is either J_1 or J_1') so that one obtains from the observed θ values $J/k_B \approx -53$ K for $CsYbZnS_3$, ≈ -45 K for $RbYbZnSe_3$, and ≈ -100 K for $CsYbZnSe_3$. These estimates of J/k_B are not consistent with that of −16 K from T_{max}. The large discrepancy between the estimates of J based on θ and on T_{max} suggests that spin–orbit coupling (SOC) effects leading to uniaxial magnetic properties[19] should not be neglected for Yb^{3+} ($S = {}^1/_2$, $L = 3$).

Furthermore, the θ value of $CsYbZnSe_3$ is inconsistent with those of $CsYbZnS_3$and $RbYbZnSe_3$. Consequently, new DC magnetic susceptibility measurements were made on $CsYbZnSe_3$. The field dependence of the magnetization

(17) Tari, A., Ed. *The Specific Heat of Matter at Low Temperatures*; Imperial College Press: London, 2003.
(18) Smart, J. S. *Effective Field Theory of Magnetism*; Saunders: Philadelphia, 1966.
(19) Dai, D.; Whangbo, M.-H. *Inorg. Chem.* **2005**, *44*, 4407–4414.

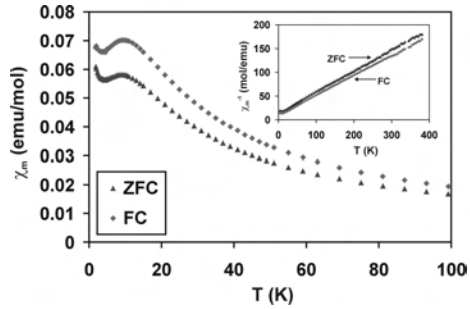

Figure 4. χ_m vs T of $CsYbZnSe_3$ for FC and ZFC data. Inset shows the plot of χ_m^{-1} vs T.

(Supporting Information) indicates that the compound is a soft magnet and displays minimal hysteresis at 2, 10, and 15 K. The temperature dependence of the molar susceptibility χ_m of $CsYbZnSe_3$ is shown in Figure 4. As expected, $CsYbZnSe_3$ exhibits a broad magnetic transition at $T_{max} \approx 10$ K as well as pronounced differences between ZFC and FC data. A plot of $\chi_m T$ versus T for both FC and ZFC data (Supporting Information) shows a steep decrease in $\chi_m T$ at $T < 100$ K. This suggests that there may be some antiferromagnetic coupling among the Yb^{3+} cations. By fitting the χ_m^{-1} versus T curves in the temperature range 50–380 K (Figure 4) in terms of the Curie–Weiss law, we obtain $\theta = -34.3(3)$ K and $\mu_{eff} = 4.26(5)$ BM for the ZFC data and $\theta = -25.4(2)$ K and $\mu_{eff} = 4.39(4)$ BM for the FC data. The present θ values for $CsYbZnSe_3$ are considerably smaller in magnitude than those reported earlier[3,4] and hence are more consistent with those for $CsYbZnS_3$ and $RbYbZnSe_3$.[3] The μ_{eff} values are much greater than the spin-only magnetic moment for $S = {}^1/_2$ (i.e., 1.73 μ_B). This indicates that the SOC effect is strong in Yb^{3+} ions. Note from Figure 4 that the zero-field-cooled (ZFC) magnetic susceptibility is lower than the field-cooled (FC) magnetic susceptibility at all temperatures. This is readily explained if the spin of Yb^{3+} is anisotropic, because an external magnetic field would have the effect of orienting the easy axes of the crystallites in powder samples of $CsYbZnSe_3$ along the direction of the magnetic field thereby enhancing the magnetic susceptibility. This in turn would make the θ value less negative because the orientation effect of the magnetic field effectively reduces the net AFM effect. This is indeed the case.

Spin Lattices. The data displayed in Figure 4 prompted us to examine the magnetic anisotropy of $CsYbZnSe_3$ by including SOC effects on the Yb^{3+} ions. Because of SOC effects, the ground-state of an isolated Yb^{3+} ion doped in a solid matrix is described by the spin–orbit coupled state $^2F_{7/2}$.[20] For this purpose, GGA+U+SOC calculations were performed for the ferromagnetic state of $CsYbZnSe_3$ with the spin moments oriented parallel to [100], [010], and [001]. Results of our GGA+U+SOC calculations are summarized in Table 2, which reveals that the spin moment of Yb^{3+} prefers to orient along [010] rather than along [100] or [001], and the orbital moment of Yb^{3+} is considerably greater than the spin moment in all three spin–orbit coupled states. Thus the spin of Yb^{3+} should be treated as highly anisotropic.

(20) Auzel, F. *J. Lumin.* **2001**, *93*, 129–135.

Table 2. Relative Energies ΔE of the Coupled States of $CsYbZnSe_3$ and the Moments of Yb^{3+} from the GGA+U+SOC Calculations

U (Ry)	spin	ΔE (meV/ unit cell)	spin moment (BM)	orbital moment (BM)
0.4	|| [100]	50	0.71	0.89
	|| [010]	0	0.73	1.26
	|| [001]	20	0.72	1.22
0.5	|| [100]	19	0.91	1.43
	|| [010]	0	0.91	1.56
	|| [001]	31	0.91	1.37

As depicted in Figure 5, it is desirable to extract three spin-exchange parameters for $CsYbZnSe_3$, namely, the intralayer interactions J_1 and J_1' discussed earlier plus the interlayer interaction J_2. The nearest neighbor Yb−Yb distances range from ≈4.08 Å (J_1'), ≈6.77 Å (J_2), and ≈5.40 Å (J_1).[4] These spin-exchange parameters can be determined by calculating the total energies of several ordered spin states of $CsYbZnSe_3$ and then equating their energy differences to the corresponding energy differences expected from the spin Hamiltonian expressed in terms of J_1 and J_2. Because there are three parameters to determine, at least four different ordered spin states should be considered in this mapping analysis.

We considered only the three ordered spin states FM, AF1, and AF2 depicted in Figure 5, because other ordered spin states involving AFM interactions along the edge-sharing ([100]) direction double the unit cell size; this makes it difficult to perform GGA+U and GGA+U+SOC calculations at the present time. Consequently, we are limited to considering only two spin-exchange parameters. Table 3 summarizes the relative total energies per chemical unit cell (i.e., per two formula units) obtained for the FM, AF1, and AF2 states of $CsYbZnSe_3$ from GGA+U calculations as well as GGA+U+SOC calculations with the spin moment of Yb^{3+} oriented along [010]. The total energies of the three ordered spin states increase in the order AF2 < FM < AF1. The energy differences among these states obtained from the GGA+U calculations are small but are well above the threshold of the energy convergence (i.e., 10^{-5} Ry = 0.14 meV). In contrast, those obtained from the GGA+U+SOC calculations are considerably larger.

To extract the values of J_1 and J_2 from the above electronic structure calculations, we express the total spin-

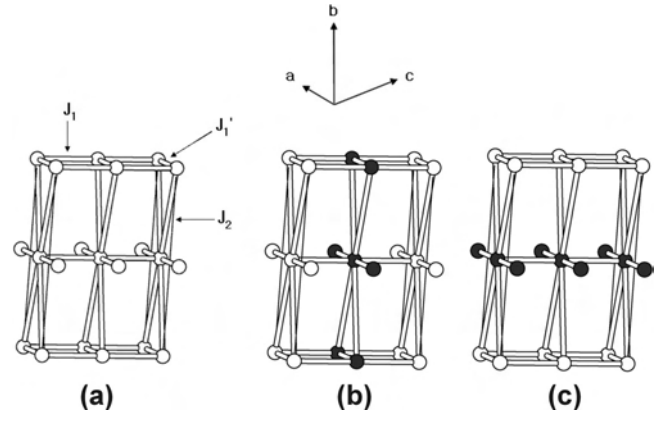

Figure 5. Spin arrangements of the Yb^{3+} ions in the (a) FM, (b) AF1, and (c) AF2 states of $CsYbZnSe_3$. The empty and filled circles represent up-spin and down-spin Yb^{3+} sites, respectively.

Table 3. Calculated Relative Energies ΔE (in meV/unit cell) of the FM, AF1, and AF2 States and Spin-Exchange Parameters for $CsYbZnSe_3$

U (Ry)	method	FM	AF1	AF2	J_1/k_B (K)	J_2/k_B (K)
0.2	GGA+U	3.5	15	0	1.3	−1.1
	GGA+U+ SOC[a]	86.4	94	0	2.8	−15.7
0.4	GGA+U	6.1	9.7	0	4.2	−0.6
	GGA+U+ SOC	4.7	15.1	0	3.8	−0.9
0.5	GGA+U	1.3	2.3	0	0.4	−0.2
	GGA+U+ SOC	32.8	46.9	0	5.1	−5.9

[a] In the GGA+U+SOC calculations for the FM, AF1, and AF2 states the spin direction was oriented along [010].

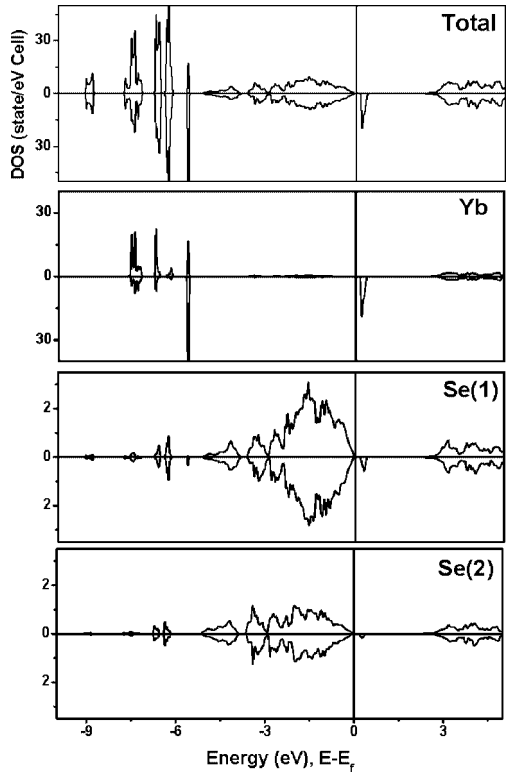

Figure 6. Total and partial DOS plots of $CsYbZnSe_3$ obtained from the GGA+U+SOC calculations with $U = 0.5$ Ry.

exchange interaction energies of the three ordered spin states in terms of the Ising spin Hamiltonian

$$\hat{H} = -\sum_{i<j} J_{ij}\hat{S}_{iz}\hat{S}_{jz} \tag{3}$$

where J_{ij} (= J_1, J_1', or J_2) is the spin-exchange parameter for the spin-exchange interaction between the spin sites i and j, whereas $\hat{S}_{iz}$ and $\hat{S}_{jz}$ are the z components of the spin angular momentum operators at the spin sites i and j, respectively. Then, by applying the energy expressions obtained for spin dimers with N unpaired spins per spin site (in the present case, $N = 1$),[21,22] the total spin-exchange energies per chemical unit cell of the FM, AF1, and AF2 states are written as

$$E_{FM} = (-4J_1 - 8J_2 - 4J_1')N^2/4 \tag{4a}$$

$$E_{AF1} = (+4J_1 - 8J_2 - 4J_1')N^2/4 \tag{4b}$$

$$E_{AF2} = (-4J_1 + 8J_2 - 4J_1')N^2/4 \tag{4c}$$

The above equations lead to

$$J_1 = (E_{AF1} - E_{FM})/2N^2 \tag{5a}$$

$$J_2 = (E_{AF2} - E_{FM})/4N^2 \tag{5b}$$

Therefore, the values of J_1 and J_2 are obtained by replacing the energy differences on the right side of eq 5 with the corresponding energy differences from the GGA+U calculations. (Note that the value of J_1' cannot be extracted from the three states FM, AF1, and AF2.) The results of this mapping analysis are summarized in Table 3, which shows that the intralayer corner-sharing spin exchange J_1 is weakly ferromagnetic (FM), whereas the interlayer spin exchange J_2 is weakly AFM. In general, DFT electronic structure calculations tend to overestimate the magnitudes of spin-exchange interactions by a factor of up to 4,[21a,22] so the actual values of J_1 and J_2 are likely to be smaller than those calculated. Therefore, to explain the observed low-dimensional AFM behavior of $CsYbZnSe_3$ with $T_{max} \approx 10$ K and $\theta \approx -34$ K (ZFC), we conclude that the spin exchange along the edge-sharing direction (i.e., [100]) is AFM and dominates over J_1 and J_2, although we were unable to estimate it directly by GGA+U/GGA+U+SOC calculations owing to the computational task involved.

As we discussed above, the spin lattice appropriate for $CsYbZnSe_3$ should be a uniform AFM chain with anisotropic spin. Given that the ground state of Yb^{3+} ($S = {}^1/_2$, $L = 3$) is $^2F_{7/2}$,[20] the spin of the Yb^{3+} ion can be uniaxial if the ground state is well separated from its excited state. [19] However, this may not be the case because the split of f-electron states by the crystal field is generally weak. Thus, one may suppose that the magnetic properties of $CsYbZnSe_3$ can be strongly anisotropic, if not uniaxial. For the sake of simplicity, let us assume that the spin of Yb^{3+} is an Ising spin so that the magnetic properties of $CsYbZnSe_3$ are described by an Ising uniform AFM chain model. When measured with magnetic field applied along the direction parallel (||) and perpendicular ($\perp$) to the chain direction, the corresponding magnetic susceptibilities ($\chi_{||}$ and $\chi_\perp$, respectively) have a maximum at $T_{||max}$ and $T_{\perp max}$, respectively. These temperatures are related to the spin exchange J as follows[23]

$$k_B T_{||max}/|J| = 0.5 \tag{6a}$$

$$k_B T_{\perp max}/|J| \approx 0.5 \tag{6b}$$

The magnetic susceptibility χ_{obs} observed for powder samples of such an anisotropic chain is related to $\chi_{||}$ and $\chi_\perp$ as

(21) (a) Dai, D.; Whangbo, M.-H. *J. Chem. Phys.* **2001**, *114*, 2887–2893. (b) Dai, D.; Whangbo, M.-H. *J. Chem. Phys.* **2003**, *118*, 29–39.

(22) (a) Dai, D.; Koo, H.-J.; Whangbo, M.-H. *J. Solid State Chem.* **2003**, *175*, 341–347. (b) Dai, D.; Whangbo, M.-H.; Koo, H.-J.; Rocquefelte, X.; Jobic, S.; Villesuzanne, A. *Inorg. Chem.* **2005**, *44*, 2407–2413.

(23) (a) Fisher, M. E. *J. Math. Phys.* **1963**, *4*, 124–135. (b) Fisher, M. E. *Physica* **1960**, *26*, 618–622.

$$\chi_{obs} = (\chi_{||} + 2\chi_{\perp})/3 \quad (7)$$

According to eqs 6a and 6b, $T_{\perp max} \ll T_{||max}$ for a given $|J|$. Thus from eq 7, when $T_{max} \approx 10$ K, the maximum in the χ_{obs} versus T plot (Figure 4) should be close to $T_{\perp max}$. Therefore, by using $T_{\perp max} \approx 10$ K in eq 6b, we estimate $J \approx -50$ K. This value of J is consistent with the one estimated from the Weiss temperature (i.e., $J/k_B \approx 2\theta$); $J/k_B \approx -53$ K for $CsYbZnS_3$, -45 K for $RbYbZnSe_3$, and -68 K (ZFC) and -50 K (FC) for $CsYbZnSe_3$. This consistency strongly suggests that an Ising uniform AFM chain model is appropriate not only for $CsYbZnSe_3$ but also for $CsYbZnS_3$ and $RbYbZnSe_3$.

Figure 6 shows plots of the total and partial density of states (DOS) obtained for $CsYbZnSe_3$ from GGA+U+SOC calculations with $U = 0.5$ Ry. The valence band given by the Se 4p orbitals is separated by an energy gap of ~0.2 eV from the conduction band given by the Yb 4f orbitals. The lowest-lying conduction band is made up of essentially unoccupied Yb 4f orbitals mixed with Se 4p orbitals. The partial DOS plot shows that the edge-sharing Se atoms [i.e., Se(1) atoms] contribute considerably more to the unoccupied Yb 4f band than do the corner-sharing Se atoms [i.e., the Se(2) atoms]. This is consistent with the conclusion that the spin exchange along the edge-sharing ([100]) direction is substantially AFM.

It remains puzzling why the isostructural compound $CsYbMnSe_3$, which contains the magnetic ion Mn^{2+} in addition to Yb^{3+}, has a broad transition at $T_{max} \approx 10$ K and a strongly negative Weiss constant of $\theta = -89.9$ K. [3] Contrast this behavior to that of the isostructural compound $CsYbCoS_3$,[5] which also contains two different magnetic ions. It shows a sharp AFM transition at ~2.7 K and has a Weiss constant of $\theta = -102.5$ K. In $CsYbMnSe_3$ the large negative value of θ implies a substantial AFM spin exchange, presumably between adjacent Yb^{3+} and Mn^{2+} ions that are separated by only 3.4874(5) Å. Thus, its spin lattice is different from the Ising uniform AFM chain found in the $AYbZnQ_3$ compounds. Further studies are necessary to understand this puzzling feature of $CsYbMnSe_3$.

Acknowledgment. The work at Northwestern University was supported in part by the Department of Energy BES Grant ER-15522. Use was made of the Central Facilities supported by the MRSEC program of the National Science Foundation (DMR05-20513) at the Materials Research Center of Northwestern University. The work at North Carolina State University was supported by the Office of Basic Energy Sciences, Division of Materials Sciences, U.S. Department of Energy, under Grant DE-FG02-86ER45259.

Supporting Information Available: Plots showing magnetization (M) vs field (H) at 2, 10, and 15 K and $\chi_m T$ vs T for FC and ZFC data for $CsYbZnSe_3$. This material is available free of charge via the Internet at http://pubs.acs.org.

IC701961F